MONITORING COMPOSITES WITH OPTICAL FIBER SENSOR SYSTEMS

Richard S. Parnas, Joy P. Dunkers, and Raymond A. Neff
Polymers Division
National Institute of Standards & Technology
Gaithersburg, MD 20899

Abstract

An inexpensive optical fiber has been interfaced with high-speed fluorescence and near infrared spectrometers to provide real-time monitoring of fast-reacting systems. Cure monitoring measurements were conducted in high volume fraction, glass reinforced composites with both an epoxy-amine system and a fast curing polyurethane-isocyanurate system. Optical theory was applied to understand the response of evanescent wave optical fiber sensors.

Introduction

Composite manufacturing faces a number of quality control issues. Currently, process development and quality control are typically accomplished through off-line, destructive mechanical testing of finished parts. For high volume manufacturing processes involving fast cycle times, the delay in getting feedback from off-line testing and the inability to test every part can result in large part-to-part variability and a high scrap rate.

Process disturbances arise from two principle sources, incoming material disturbances and in-process disturbances. Disturbances to the incoming material include resin degradation, moisture content, catalyst variation, reinforcement fiber misalignment, and preform size or shape variation. Although these disturbances can severely affect both the cure kinetics and flow behavior during processing, they can be identified by careful inspection. However, such inspection, especially of preforms, can result in rejection rates over 50%. In-process disturbances arise from sources such as seasonal and diurnal temperature and humidity fluctuations, mixing of multiple component systems, especially small amounts of catalysts, and equipment aging. Some of these are predictable and some are random.

In established chemical manufacturing industries, process control methodologies are well known to mitigate the effects of such disturbances [1]. A typical process control structure is schematically illustrated in Figure 1. Typical composites processing equipment includes base-level control of temperatures, pressures, and in some cases flows. Since the disturbances outlined above often do not affect the basic process variables (temperature, pressure, flow), controlling just the basic process variables is inadequate.

Our work has focused on improving on-line process monitoring (the sensors box in Figure 1) to provide high-level control structures the critical information required for control decisions. In previous work [2,3], we introduced evanescent wave optical fiber fluorescence and infrared systems to monitor cure during liquid composite molding. In this paper we present example results and a brief discussion of the optical theory used to interpret the sensor signals.

Experimental

The fluorescence monitoring system uses a polarity-sensitive dye, 4-(N, N-dimethylamino)-4'-nitrostilbene (DMANS), dissolved in one resin component at a concentration of 4.8×10^{-4} M. The emission spectrum of DMANS exhibits a large wavelength shift (45 nm) to shorter wavelengths during resin cure. The detector is a 0.25 m imaging spectrograph, equipped with a CCD camera. The beam directing optics have recently been miniaturized to a small closed unit that mounts onto a miniature air-cooled laser unit. The spectral acquisition time varied between 200-500 ms for evanescent wave experiments and between 50-100 ms for distal end experiments. Spectra were acquired approximately once every minute for the epoxy-amine system and once every 5 s for the polyurethane system.

The NIR monitoring system uses a Fourier transform infrared (FT-IR) spectrometer equipped with a quartz-tungsten-halogen white light source, calcium fluoride beamsplitter, and a mercury-cadmium-telluride (MCT-A) detector. Spectral acquisition and delay time were automated using available software. One hundred scans were co-added at a resolution of 16 cm^{-1} with a time delay of 5.7 min for the epoxy system. Each spectrum took 36.5 s to acquire at a mirror velocity of 1.90 cm/s. For the polyurethane resin system, fifty scans were co-added at a resolution of 16 cm^{-1} with a 30 s delay time, and each spectrum took 4.44 s to acquire at a mirror velocity of 3.16 cm/s. The sensor for near IR used three 130 μm diameter optical fibers to promote signal-to-noise by increasing the energy throughput. In both the NIR and fluorescence systems, the optical fibers consisted of a silica glass containing 45 weight percent lead oxide to increase the refractive index, permitting evanescent wave sensing.

Two chemical systems were used, DGEBA epoxy

cured with a variety of aliphatic and aromatic amine hardeners, and a polyurethane system of diisocyanate/diol catalyzed by triethylenediamine (~ 3 min gel time). In both cases, the reaction mixture was injected into a preheated mold containing approximately 50% by volume unidirectional E-glass fibers.

Example Results

Graphs of the position of the fluorescence peak maximum (λ_{max}) as a function of time for the epoxy system at 90°C and 110°C are shown in Figure 2. Distal end experiments are represented by the solid lines and circles and evanescent wave experiments by the dotted lines and squares. From a statistical analysis, the uncertainty in λ_{max} is approximately 1 nm. Note that the position of the peak maximum is a function of both the extent of cure and temperature [2]. For data taken 110°C, λ_{max} reaches its final value faster than at 90°C due to changes in reaction kinetics. However, the final λ_{max} is higher at the higher temperature due to the temperature shift.

The data initially indicate that the cure proceeds slower for the evanescent wave measurements (□) than for the distal measurements (○), suggesting that the evanescent sampling geometry measured differences occurring at the resin/fiber interface. However, a second order background correction of the evanescent wave spectra (Δ) reveals that the evanescent wave and distal end spectra are identical. Thus, the reaction chemistry is identical within the sampling volumes of the evanescent wave and distal end measurements. A model of an epoxy-amine system with carbon fibers [4] predicted interfacial effects within a region restricted to 10 nm from the fiber surface. Since the optical theory described below predicts that the evanescent wave measurement samples a region out to at least 100 nm from the fiber surface, we would not expect to observe the interfacial chemistry.

The near IR spectra of curing epoxy in the mold are shown in Figure 3 at several times. Figure 4 displays the consumption of the oxirane (6070 cm^{-1}), primary and secondary amines (6650 and 6580 cm^{-1}), and primary amine (5049 cm^{-1}), and secondary amine (calculated) as well as mold temperature. All peak areas were normalized to the internal standard band at 5655 cm^{-1}, a methylene overtone band, for the conversion calculation. From this data, all of the primary amine is consumed within 40 min which also corresponds to the maximum in the amount of secondary amine.

Fluorescence data for the polyurethane system are shown in Figure 5. The reaction was easily followed even though the gel point occurred in only 3 min. A pronounced change in the λ_{max}, and a maximum in peak intensity coincide with the observed gel point at 3 min. The intensity decrease primarily results from the reaction exotherm, which coincides with gelation of the resin (due to a decrease in heat capacity). We typically observe a decrease in the quantum efficiency of DMANS with increasing temperature in the cured polymer. Photobleaching of the dye may also contribute to the intensity decrease since diffusion in the cured polymer is very slow compared with the liquid resin.

The near IR spectra of the reacting polyurethane are shown in Figure 6. These spectra are scaled to the internal standard band at 5970 cm^{-1}, which is an aromatic C-H stretching first overtone [5]. The resin reacts so rapidly that, at 4 s in the sample cell, N-H groups are already forming as evidenced by the peak formation at 6700 cm^{-1}. The peak at 6995 cm^{-1} is a -OH stretching overtone that is consumed within 1 minute. Peaks at 5780 and 5672 are aliphatic -CH stretching overtones. The multiple peak near 5332 cm^{-1} is partially due to the -C=O second overtone stretch of the isocyanate [6] and decreases in intensity with time when compared to the internal standard peak at 5970 cm^{-1}.

It can be qualitatively seen from the spectra of the reacting material in Figure 6 that the carbonyl peak from the isocyanate is consumed much slower than the hydroxyl peak. The formation of the urethane linkage is highly favored at these temperatures and with the catalyst, and it is due to the non-stoichiometic nature of this reaction that the isocyanurate is formed [7].

Optical Theory and Calculations

The optical theory is presented for the case of the fluorescence sensor. When an optical fiber is immersed into a fluid containing fluorescent dye, it is possible to excite the fluorescence with a beam propagating in the fiber and collect some of the fluorescence with the same fiber [2,8]. Starting from Marcuse [9], we can compute the power of the coupled fluorescence radiation propagating back up the fiber core as P^f_{core},

$$P^f_{core} = \frac{1}{16P_o} \sum_{modes} \int S|E^f_{\nu,\rho}|^2 dV \qquad (1)$$

where S is the source strength of the fluorescent radiation, $[E^f_{\nu,\rho}]$ is the electric field intensity of the evanescent tail of the fluorescence mode (ν,ρ) propagating in the fiber, P_o is a units conversion factor, and the integral is carried out over the volume outside the fiber where fluorescence occurs. The evanescent field intensity coupled with each propagating mode in a fiber of radius a is expressed, in the limit of the weak guidance approximation [10], as

$$|E_{\nu,\rho}| = 2AJ_\nu(\kappa_{\nu,\rho}a)\frac{K_\nu(\gamma_{\nu,\rho}r)}{K_\nu(\gamma_{\nu,\rho}a)} \qquad r>a \quad (2)$$

where J_ν is the Bessel function of order ν, K_ν is the

modified Bessel function of order v, A is an amplitude coefficient, and κ and γ are the propagation constants for each mode [10]. An important point to note is the propagation constants for the fluorescent radiation are different than the propagation constants for the excitation radiation due to their different wavelengths. Consequently, the number of propagating modes of excitation and fluorescent radiation will also be different.

The source strength S couples the fluorescence radiation to the excitation. If we compute the Poynting vector for the flow of power in the evanescent waves and assume spherically symmetric fluorescence, then S is

$$S = \frac{\lambda\alpha\chi}{\omega\mu_o}\left(\frac{\epsilon_o}{\mu_o}\right)^{1/2}\sum_{v,\rho}|E^e_{v,\rho}|^2 \qquad (3)$$

given in terms of the modes of the excitation radiation, α is the absorptivity of the medium and χ is the fluorescence quantum efficiency. This expression also assumes that the emitted fluorescence power from a volume element is linearly proportional to the excitation power impinging on the surface of that same volume element [11].

Combining Eqs. (1) and (3) gives an expression for the fluorescence power recovered in the fiber

$$P^f_{core} = \frac{\pi\lambda\alpha\chi(\epsilon_o/\mu_o)^{\frac{1}{2}}L}{8P_o\omega\mu_o}\sum_{v,\rho}^{f}\int\left[\sum_{v,\rho}^{e}|E^e_{v,\rho}|^2\right]|E^f_{v,\rho}|^2 r\,dr \qquad (4)$$

The two summation symbols are each labeled with either an "e" or an "f" to indicate clearly that the summations are to be conducted over either the excitation or the fluorescence modes, respectively.

Example calculations with Eq. (4) are shown in Figure 7. The normalized fluorescence power propagating in the fiber is plotted as a function of the radial distance away from the fiber from which the power was collected. Thus, as the radial distance extends to infinity, the normalized collected power approaches unity.

The calculations presented were performed with several values of the resin refractive index. In all cases, at least 20 propagating modes of excitation and fluorescence radiation existed. Early in the resin cure when the resin refractive index is low, most of the signal is collected from a region very close to the fiber surface, perhaps from within 100 nm of the fiber. However, as the resin refractive index approaches the fiber index, the region of signal collection extends significantly until at least a 250 nm distance from the fiber is sampled.

These sampling depths are significantly less than the 1 or 2 μms sampled in infrared ATR investigations for two reasons [12]. First, the excitation wavelength of 488 nm is much shorter than IR wavelengths, resulting in a shorter depth of penetration of the excitation beam. Note, however, that the evanescent field around a cylindrical fiber decays according to the Bessel function given in Eq.(2) rather than a simple exponential as does the field near the flat plate waveguides used in ATR work. Nevertheless an effective depth of penetration of approximately 0.5 to 0.75 μms was computed for the excitation field for comparison to the depths of penetration quoted for ATR. Second, the coupling of the excitation field to the fluorescence field results in a further compression of the sensing region, as indicated by the multiplication of the squares of the excitation and fluorescence fields in Eq. (4).

This model can help interpret the evanescent wave data illustrated in Figure 2 that was collected during the molding of a glass/epoxy composite plaque. In the epoxy system, comparisons were made and significant differences were observed between the apparent rate of cure when evanescent measurements were compared to distal and bulk fluorescence measurements, suggesting differences between the cure kinetics in the interphase relative to the bulk resin. However, before differences in the interphase cure kinetics can be ascribed to the resin systems, the measurement region needs to be determined accurately. The model described above provides an estimate of the sample volume with greater certainty than simple "depth of penetration" arguments based on flat plate optical analysis.

In all cases, a significant portion of the signal was collected from the region beyond 100 nm from the fiber, therefore the interfacial sensitivity of the measurement is low for the amorphous resin systems studied. That result lends credence to an alternative explanation based on spectral analysis involving second order background corrections to the collected spectra [13]. More importantly, the model allows one to explore sensor designs that may either emphasize or further diminish the interfacial sensitivity. Lastly, with some modification, a similar model under construction will enable more accurate interpretation of near infrared spectra obtained with evanescent optical fiber measurements.

Summary

High speed optical fiber sensor systems have been developed for both fluorescence and near infrared monitoring of resin cure during composites manufacturing. Both spectroscopic techniques can use the same optical fiber, although the fluorescence system has the flexibility to use standard telecommunications fiber in distal sensing mode. Both an epoxy-amine system and a faster reacting polyurethane-isocyanurate system were employed to demonstrate the improved systems.

Optical modeling indicates that the region sampled is order 100 nm in radius around the fiber for

fluorescence. This is consistent with the second order background correction used to bring the evanescent wave fluorescence results into agreement with the bulk distal results for the epoxy resin.

References

1. B. Oggunaike, *Proc. Nat.Acad.Eng. Frontiers of Eng*, Sept.1997.
2. D.L. Woerdeman, J.K. Spoerre, K.M. Flynn and R.S. Parnas, *Polymer Composites*, **18(1)**, 133 (1997).
3. J. Dunkers, K. Flynn, and R. Parnas, *Composites, Pt. A.*, **28(2)**, 163 (1996).
4. G.R. Palmese, Ph.D. Thesis, University of Delaware, 1992.
5. C. Miller, P. Edelman, and B. Ratner, *Appl. Spect.*, **44(4)**, 576 (1990).
6. C. Miller and B. Eichinger, *J. Appl. Polym Sci.*, **42**, 2169 (1991).
7. K. Schwetlick and R. Noack, *J. Chem. Soc., Perk. Trans.*, **2**, 395 (1995).
8. R.L. Levy and S.D. Schwab, *Polymer Composites*, **12(2)**, 96-101, 1991.
9. D. Marcuse, *J. Lightwave Tech.*, **6(8)**, 1273-1279, 1988.
10. D. Marcuse, *Theory of Dielectric Waveguides*, Chapman & Hall, London, 1991.
11. J.R. Lakowicz, *Principles of Fluorescence Spectroscopy*, Plenum Press, New York, 1983.
12. R.A. Shick, J.L. Koenig and H. Ishida, *Applied Spectroscopy*, **50(8)**, 1082-1088, 1996.
13. R.A. Neff, D.L. Woerdeman and R.S. Parnas, *Polymer Composites*, **18(4)**, 518 (1997).

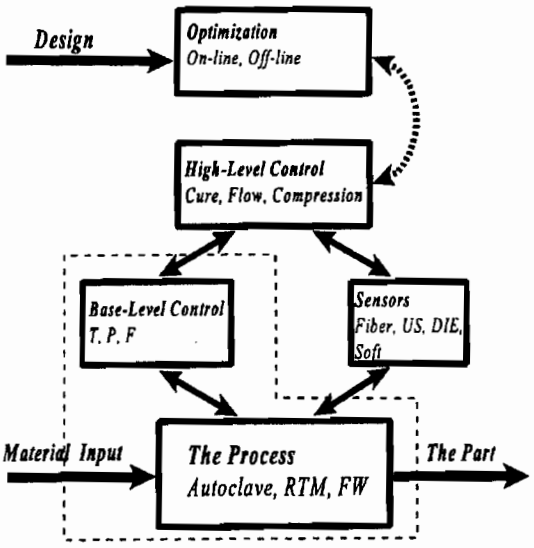

Figure 1. Control system for composites illustrating the major components, base-level control, sensors, high-level control, and optimization.

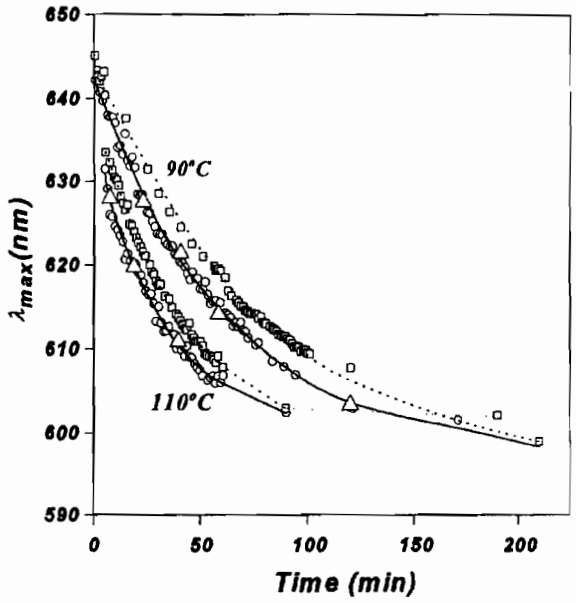

Figure 2. Wavelength position vs. time for epoxy-amine system, isothermal cure. All the distal (O) and uncorrected evanescent wave (□) measurements are shown. The large triangles (Δ) correspond to a subset of the evanescent mode data treated with a second order background correction to show that properly interpreted evanescent data are identical to the distal data.

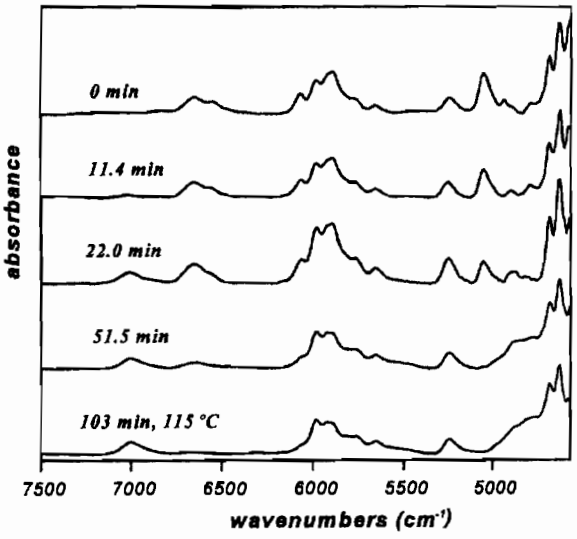

Figure 3. Near IR spectra of reacting epoxy resin at several times during a two stage cure, where the temperature was held at 90°C for 90 min and then ramped to 150°C.

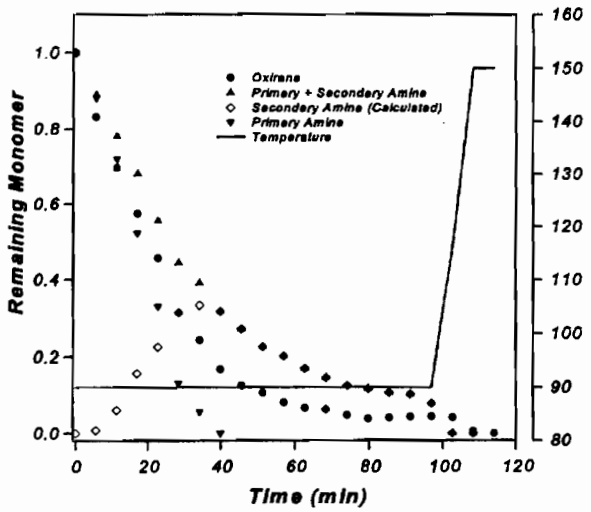

Figure 4. Plot of remaining oxirane, total amine, and primary amine obtained by near IR with an embedded fiber optic mini-bundle sensor in an RTM part. The solid line is the mold wall temperature.

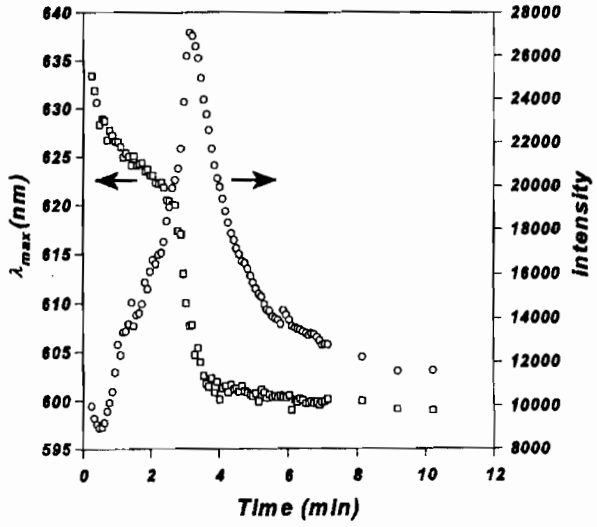

Figure 5. Peak wavelength position and fluorescence intensity during the cure of polyisocyanurate resin.

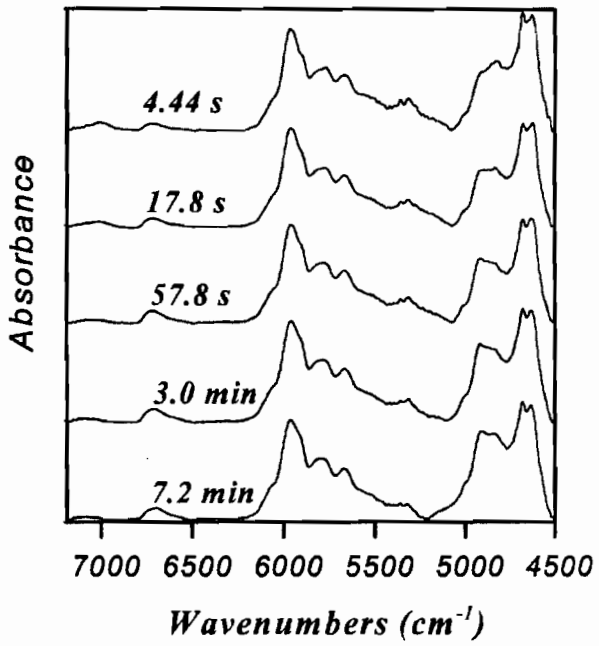

Figure 6. Near IR spectra of reacting polyisocyanurate resin at several times.

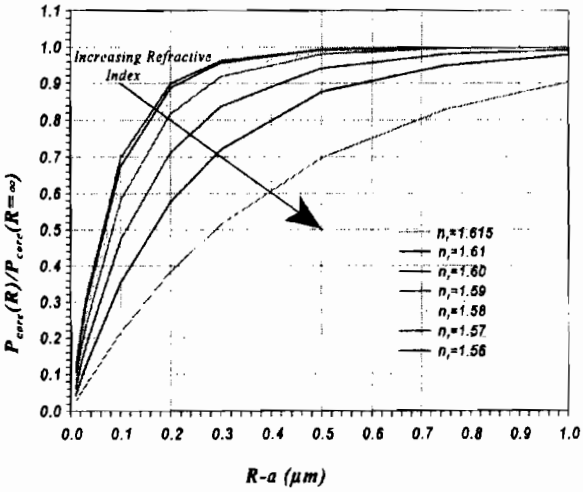

Figure 7. Cumulative fluorescence power in a fiber of index 1.617 for resins of several indices, at an excitation wavelength of 488 nm and a fluorescence wavelength of 625 nm.